# A Theoretical Investigation of the Structure and Electronic Spectra of Porphyrin Homolog Macrocycles. Hexaazacyclophane and Its Nickel and Copper Complexes

**Guillermina L. Estiú*,†,‡ and Alicia H. Jubert*,‡**

Programa QUINOR, Departamento de Química, Facultad de Ciencias Exactas, Universidad Nacional de La Plata, C.C. 962, 1900 La Plata, Argentina, and Departamento de Ciencia y Tecnología, Universidad Nacional de Quilmes, Roque Saénz Peña 180, 1876, Bernal, Argentina

**José Molina**

Departamento de Química, Facultad de Ciencias Exactas, Universidad Nacional de Salta, Buenos Aires 177, 4400, Salta, Argentina

**Juan Costamagna and Juan Canales**

Departamento de Química, Facultad de Ciencia, Universidad de Santiago, Santiago 2, Chile

**Juan Vargas**

Departamento de Química, Universidad Metropolitana de Ciencias de Educación, Santiago, Chile

*Received April 26, 1994*[⊗]

A quantum chemical study of the geometry, electronic structure, and electronic spectra of hexaazacyclophane and its Ni and Cu complexes, of major interest in the electrochemical reduction of $CO_2$, has been carried out using the INDO method, in its INDO/1 and INDO/S parametrizations. The electronic spectra were calculated using a CI-S, generating the configurations by means of a Rumer diagram technique. The calculations confirm the singlet ground state for the ligand and Ni complex, as well as the doublet ground state for the Cu one. They are planar structures of $D_{2h}$ symmetry. Although the structures are considered porphyrin homologs, the calculated spectra cannot be described in terms of Q and B (Soret) bands as in porphyrins, and no band in the visible develops for the base. Low-energy transitions are associated with d → d excitations (around 450 nm) in the Ni complex and with metal → ligand charge transfer from the HOMO $d_{xy}$ (in the 900−450 nm region) in the Cu complex, characterized by an open shell structure.

## 1. Introduction

The last decades have been marked by significant advances in the knowledge of the physical and chemical properties of metalloporphyrins and related macrocyclic transition metal complexes.[1−3] With major practical interest related to electrocatalysis[4] and photochemistry,[5] they offer the possibility of widely and selectively changing their activity by means of either the modification of the electronic characteristics of the aromatic macrocycles by programmed substitution or the selection of active or inactive metals as the centers to be chelated.

The catalytic properties are associated with electron transfer processes that involve, to different extents, $\pi$ electrons delocalized in the macrocycle, d electrons on the metal, and charge transfer transitions between them.[4] Interactions involving the metal center would be affected, on the other hand, by the nature of the ligands, which determines the ligand field strength[6] and, thence, the availability of the d electrons, which, through a balance of metal−N $\sigma$ bonding and $\pi$ back-bonding from the chelating cycle to the metal center, will determine the metal−ligand bond interactions.[7]

Porphyrinoids and related compounds are also important in photodynamic therapy, destroying efficiently malignant tissue upon red light irradiation.[8] Although the associated mechanism has not been determined unequivocally, the activity is related to the capacity of *in vivo* formation of $O_2$ ($^1\Delta_g$).[9]

Because of the importance of the electronic excitations in both charge transfer and photoactivated processes, the electronic spectra of metallo-macrocycles have always attracted major

† Universidad Nacional de Quilmes.
‡ Universidad Nacional de La Plata.
⊗ Abstract published in *Advance ACS Abstracts*, January 15, 1995.

(1) Gouterman, M. *The porphyrins*; Dolphin, D., Ed.; Academic: New York, 1978.
(2) Morgan, B.; Dolphin, D. *Struct. Bonding* **1987**, *64*, 116.
(3) Berezin, B. D. *Coordination Compounds of Porphyrins and Phthalocyanines*; J. Wiley & Sons: New York, 1981.
(4) Zagal, J. H. *Coord. Chem. Rev.* **1992**, *119*, 89.
(5) Mártire, D. O.; Jux, N; Aramendía, P. F.; Negri, R. M.; Lex, J.; Braslavsky, S. E.; Schaffner, K.; Vogel, E. *J. Am. Chem. Soc.* **1992**, *114*, 9969.
(6) Gurinovich, G. P.; Sevchenko, A. N.; Soloyev, K. N. *Spectroscopy of Clorophyll and Allied Compounds*; Nauka i tekhnika: Minsk, Russia, 1968.
(7) Ochiai, E. *Química Bioinorgánica*; Editorial Reverté: Barcelona, Spain, 1985.
(8) (a) Aramendía, P. F.; Redmond, R. W.; Nonell, S.; Schuster, W.; Braslavsky, S. E.; Schaffner, K.; Vogel, E. *Photochem. Photobiol.* **1986**, *44*, 555. (b) Redmond, R. W.; Valduga, G.; Nonell, S.; Braslavsky, S. E.; Schaffner, K.; Vogel, E.; Pramod, K.; Kocher, M. *Photochem. Photobiol. B* **1989**, *3*, 193. (c) Guardiano, M.; Biolo, R.; Jori, G.; Schaffner, K. *Cancer Lett.* **1989**, *44*, 1. (d) Milanesi, C.; Biolo, R.; Jori, G.; Schaffner, K. *Lasers Med. Sci.* **1991**, *6*, 437.
(9) Moan, J. J. *J. Photochem. Photobiol. B* **1990**, *5*, 521.

0020-1669/95/1334-1212$09.00/0 

attention.[10-16] From the characteristic intense Soret band (~400 nm) in the electronic spectra of metalloporphyrins, together with lower intensity bands in the visible region, noticeable changes develop according to the characteristics of the macrocycle, which are able to be correlated with several properties. Besides, it has been established that the activity of the porphyrin catalysts is determined primarily by the choice of the metal and axial ligands as well as the electronic properties of the macrocycles and steric factors generated by them.[17]

After the early comparison of porphyrins and phthallocyanines in their properties and reactivity, much effort has been devoted to the synthesis and characterization of different N-dentate chelating macrocycles. Porphycenes,[8,18] sapphyrins,[19] and texaphyrins[20] can be mentioned among others. However, little is known about the properties of macrocyclic compounds derived from 1,10-phenanthroline.[21-26] Since these compounds can be considered relatives of phthallocyanines and porphyrins, they have potentially interesting chemical properties as redox catalysts.

The electronic spectra of the different chelating macrocycles and their metal complexes not only render a characterization of their structure but also allow the justification of, after a thorough study of the origin of the electronic features, changes in the reactivity toward processes that involve electronic excitations. From the analysis of the low-energy electronic transitions and the appropriate assignments of the molecular orbitals involved, the role of the metal d and ligand $\pi$ orbitals can be understood and the way to improve a given photochemical or electrochemical effect, working on the availability of either the d or $\pi$ electrons, decided.

Structural changes usually involve substitution on the pyrrol rings or the introduction of aza bridges keeping the tetrapyrrol basic skeleton. However, armed by the knowledge of the effect of the structure of the proximal N base upon the differential affinity of heme complexes for oxygen and CO,[27] some synthetic non-pyrrolic tetraaza and hexaaza macrocycles have been studied as porphyrin models.[28-30] Among others, macrocycles similar to the azacyclophanes show catalytic activity in some processes related to energy storage and/or to the obtention of fuels.[31-34] For example, the large overpotential required for electrode reactions to proceed at an appropriate rate is an unquestionable technical problem which has been addressed by adding some catalysts,[35-39] among which tetraaza macrocyclic and related complexes of cobalt and nickel have recently been successfully used.[40-43] Aza macrocycles derived from 1,10-phenanthrolines, with an extended $\pi$-electronic system, are, thence, promising catalysts.

For the particular case of the hexaazacyclophane base, and its copper, nickel, and cobalt complexes, the electronic and stereochemical structures are known from XPS and magnetic susceptibility measurements.[28] The metal complexes are characterized by a square planar structure of the ligand around the central ion, the hexaaza macrocycle nickel complex being diamagnetic and the copper complex paramagnetic. Preliminary studies[30] show, on the other hand, an important redox activity and efficiency to catalyze the $CO_2$ electroreduction reaction, which is known to be associated with the energy of the electronic excitations.

It is important, thence, to determine whether ligand → ligand, metal d → d, metal → ligand, or ligand → metal excitations are more relevant for the above mentioned reactions.

There is a considerable body of information describing the structural and spectroscopic properties of hexaazacyclophane macrocycles and their metal complexes. In the present study two aspects have been investigated: the ground state structure of the macrocycle and its metal complexes and the origen of the transitions developed in the electronic spectra. To this end, we have performed self-consistent field *(SCF)* and configuration interaction *(CI)* calculations, using the semiempirical intermediate neglect of differential overlap method,[44] either parametrized for geometry[45,46] (*INDO/1*, structure calculations) or for spectroscopy[47,48] (*INDO/S*). Comparisons with the porphyrin homologs are included.


(10) Gouterman, M. *J. Mol. Spectrosc.* **1961,** *6,* 138.
(11) Caughey, W. S.; Deal, R. M.; Weiss, C.; Gouterman, M. J. *Mol. Spectros.* **1965,** *16,* 451.
(12) Edwards, W. D.; Weiner, B.; Zerner, M. C. *J. Am. Chem. Soc.* **1986,** *108,* 2196.
(13) Cory, M. G.; Zerner, M. C. *Chem. Rev.* **1991,** *91,* 813.
(14) Du, P.; Axe, F. U.; Loew, G.; Canuto, S.; Zerner, M. C. *J. Am. Chem. Soc.* **1991,** *113,* 8614.
(15) Clark, P. A.; Jansonius, J. N.; Mehler, E. L. *J. Am. Chem. Soc.* **1993,** *115,* 1894.
(16) Gold, A.; Jayaraj, K.; Doppelt, P.; Weiss, R.; Chottard, G.; Bill, E.; Ding, X.; Trautwein, A. X. *J. Am. Chem. Soc.* **1988,** *110,* 5756.
(17) Sparks, L. D.; Medforth, C. J.; Park, M. S.; Chamberlain, J. R.; Ondrias, M. R.; Senge, M. O.; Smith, K. M.; Shelnutt, J. A. *J. Am. Chem. Soc* **1993,** *115,* 581.
(18) Vogel, E. *Pure Appl. Chem.* **1990,** *62,* 557.
(19) Sessler, J. L.; Cyr, M. J.; Burrell, A. K. *Synlett 1991,* 127.
(20) Sessler, J. L.; Murai, T.; Hemmi, G. *Inorg. Chem.* **1989,** *28,* 3390.
(21) Melson, G. A. In *Coordination Chemistry of Macrocyclic Compounds*; Melson, G. A., Ed.; Plenum Press: New York, **1979.**
(22) Grant, J. L.; Goswami, K.; Otvos, L. O.; Calvin, M. *J. Chem. Soc., Dalton Trans.* **1987,** 2105.
(23) Ferraudi, G. *Coord. Chem. Rev.* **1981,** *36,* 45 and references therein.
(24) Ferraudi, G. *Inorg. Chem.* **1979,** *18,* 3230; **1980,** *19,* 438.
(25) Muralidharan, S.; Ferraudi, G. *Inorg. Chem.* **1981,** *20,* 2306.
(26) Endicott, J. F.; Durham, B. In *Coordination Chemistry of Macrocycles Complexes*; Melson, M. A., Ed.; Plenum Press: New York, 1979; Chapter 6 and references therein.
(27) Chang, C. K.; Traylor, T. G. *J. Am. Chem. Soc.* **1973,** *95,* 8477.
(28) Seno, M.; Tsuchiya, S.; Ogawa, S. *J. Am. Chem. Soc.* **1977,** *99,* 3014.
(29) Costamagna, J.; Canales, J.; Vargas, J.; Camalli, M.; Caruso, F.; Rivarola, E. *Pure Appl. Chem.* **1993,** *65,* 1521.
(30) Costamagna, J.; Canales, J.; Vargas, J; Alvarado, A.; Ferraudi, G. *J. Ind. Chem. Soc.*, in press.
(31) Eisemberg, R.; Hendriksen, D. E. *Adv. Catal.* **1979,** *28,* 79.
(32) Sneeden, R. P. In *Comprehensive Organometallic Chemistry;* Wilkinson, G., Stone, F. G. A., Abel, E. W., Eds.; Vol 8. Pergamon Press: New York, 1982; Vol. 8.
(33) Bohr, A. In *Carbon Dioxide activation by metal complexes;* VCH: New York, 1988.
(34) Darensbourg, D. J.; Kudaroski, R. A. *Adv. Organomet. Chem.* **1983,** *22,* 129.
(35) Beley, A.; Collin, J.; Ruppert, R.; Sauvage, J. *J. Am. Chem. Soc* **1986,** *108,* 17.
(36) Meshitsuka, S.; Ichikawa, M.; Tamaru, K. *Chem. Commun.* **1974,** 158.
(37) Hiratsuka, K.; Takahashi, K.; Sasaki, H.; Toshima, S. *Chem. Lett.* **1977,** 1137.
(38) Takahashi, K.; Hiratsuka, K; Sasaki, H.; Toshima, S. *Chem. Lett.* **1979,** 305.
(39) Fisher, B.; Eisenberg, R. *J. Am. Chem. Soc.* **1980,** *102,* 7363.
(40) Lehn, M.; Ziessel, R. *Proc. Natl. Acad. Sci. U.S.A.* **1982,** *79,* 701.
(41) Hawecker, J.; Lehn, J. M.; Ziessel, R. *J. Chem. Soc., Chem. Commun.* **1985,** 56.
(42) Kutal, C.; Weber, M. A.; Ferraudi, G.; Geiger, D. *Organometallics* **1985,** *4,* 2161.
(43) Sullivan, B. P.; Meyer, T. J. *J. Chem. Soc., Chem. Commun.* **1984,** 1244.
(44) (a) Pople, J. A.; Beveridge, D. L.; Dobosh, P. A. *J. Chem. Phys.* **1967,** *47,* 2026. (b) Ridley, J. E.; Zerner, M. C. *Theor. Chim. Acta* **1976,** *42,* 223. (c) Bacon, A. D.; Zerner, M. C. *Theor. Chim. Acta* **1979,** *53,* 21.
(45) Head, J. D.; Weiner, B.; Zerner, M. C. *Int. J. Quant. Chem.* **1988,** *33,* 177.
(46) Anderson, W. P.; Cundari, T. R.; Zerner, M. C. *Int. J. Quant. Chem.* **1991,** *34,* 31.
(47) Zerner, M. C.; Loew, G.; Kirchner, R. F.; Mueller-Westerhoff, U. T. *J. Am. Chem. Soc.* **1980,** *16,* 589.
(48) Zerner, M. C. In *Reviews in Computational Chemistry*; Lipkowitz, K. B., Boyd, B. D., Eds.; VCH Publishers: New York, 1990; Vol. 2.

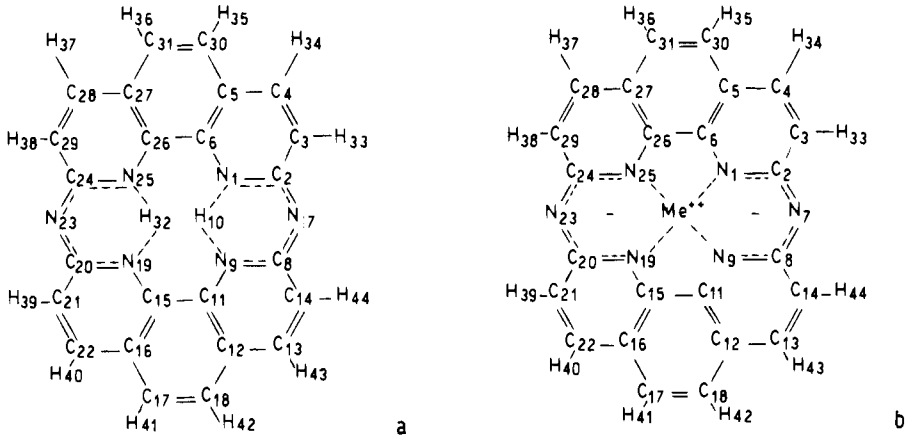


**Figure 1.** (a) Compound 1: Hexaazacyclophane base. (b) Compound 2: Metal complexes, Me = Ni, Cu. We have adopted the convention used in ref 22 to indicate the delocalization of the electrons, showing that both H atoms in the base, as well as the metal in the complex, are equally shared by both cyclophane moieties. The delocalization is actually extended to the whole structure. Interatomic distances $r$ (Å): (a) $r_{1-2} = 1.370$, $r_{2-3} = 1.428$, $r_{3-4} = 1.362$, $r_{4-5} = 1.430$, $r_{5-6} = 1.412$, $r_{1-6} = 1.387$, $r_{27} = 1.363$, $r_{1-10} = 1.206$, $r_{6-26} = 1.434$, $r_{5-30} = 1.425$, $r_{30-31} = 1.369$, $r_{3-33} = 1.096$, $r_{4-34} = 1.097$, $r_{30-35} = 1.096$; (b) $r_{1-2} = 1.366$, $r_{2-3} = 1.431$, $r_{3-4} = 1.363$, $r_{4-5} = 1.432$, $r_{5-6} = 1.405$, $r_{1-6} = 1.387$, $r_{2-7} = 1.359$, $r_{1\text{-Me}} = 1.839$, $r_{6-26} = 1.438$, $r_{5-30} = 1.424$, $r_{30-31} = 1.370$, $r_{3-33} = 1.096$, $r_{4-34} = 1.117$, $r_{30-35} = 1.112$. Local charge densities ($\delta$) on the atomic centers: (a) Charges are given for the dianion: $\delta_1 = -0.337$, $\delta_2 = 0.231$, $\delta_3 = -0.069$, $\delta_4 = -0.031$, $\delta_5 = -0.048$ $\delta_6 = 0.121$, $\delta_7 = -0.516$, $\delta_{30} = -0.080$, $\delta_{33} = -0.013$, $\delta_{34} = -0.012$, $\delta_{35} = -0.005$; (b) Ni complex, $\delta_{Ni} = -0.038$, $\delta_1 = -0.170$, $\delta_2 = 0.271$, $\delta_3 = -0.033$, $\delta_4 = 0.022$, $\delta_5 = -0.005$, $\delta_6 = 0.098$, $\delta_7 = -0.437$, $\delta_{30} = -0.035$, $\delta_{33} = 0.034$, $\delta_{34} = 0.026$, $\delta_{35} = 0.021$; Cu complex, $\delta_{Cu} = 0.144$, $\delta_1 = -0.205$, $\delta_2 = 0.265$, $\delta_3 = -0.032$, $\delta_4 = 0.022$, $\delta_5 = -0.004$, $\delta_6 = 0.088$, $\delta_7 = -0.437$, $\delta_{30} = -0.034$, $\delta_{33} = 0.035$, $\delta_{34} = 0.026$, $\delta_{35} = 0.021$.

## 2. Methodology

**2.1. Experimental Methods.** Synthetic methods for azacyclophanes were reported early by Ogawa, as a cumbersome multistep synthesis which produce the ligands with extremely low yield, i.e. <1%.[49,50] This synthetic problem has limited the research on these compounds to the determination of a few spectra.[51,52] We have introduced some modifications, related to the rigorous exclusion of moisture from the reactions and the use of separation chromatographic techniques.[30] Commercial 1,10-phenanthroline was used without further purification. Methylation, oxidation to phenanthrolone, and chloration lead to 2,9-dichloro-1,10-phenanthroline, whose further ammonolysis brought 2,9-diamino-1,10- phenanthroline.[53] Finally, through a condensation between 2,9-dichloro- and 2,9-diamino-1,10-phenanthroline, the hexaaza macrocycle (Figure 1a) was obtained. The synthesis of the Ni(II) and Cu(II) complexes (Figure 1b) is described elsewhere.[30] Elemental analysis of metal, carbon, nitrogen, and hydrogen for the complexes synthesized are in agreement with a 1:1 metal to ligand stoichiometry within an error range of 5%.

UV−vis spectra (Figure 2) were recorded on a Karl Zeiss Model DMR22 and on a Perkin-Elmer Model Cary-17. No substantial solvent effects were found in the electronic spectra of the Ni(II) complex, while the Cu(II) one shows noticeable changes. This fact has been previously observed[54] and explained in terms of the molecular orbitals involved in the transitions.[55,56] Common features develop in the high-energy region. The lower energy bands, which appear after chelation, are different for the Ni and Cu complexes.

The synthesis and IR, UV−vis, $^1$H-NMR, and electrochemical characterization of new complexes of Ni(II) and Cu(II) with macrocycle ligands derived from azacyclophanes synthesized from 1,10-phenanthroline are being published separately.[30]

**2.2. Computational Details.** In this paper we report the results of the application of the intermediate neglect of differential overlap method (ZINDO package)[57] to analyze the electronic spectra and the structure of the lower lying states of the hexaazacyclophane base and its Ni and Cu complexes (Figure 1a,b) at both the RHF and ROHF levels.

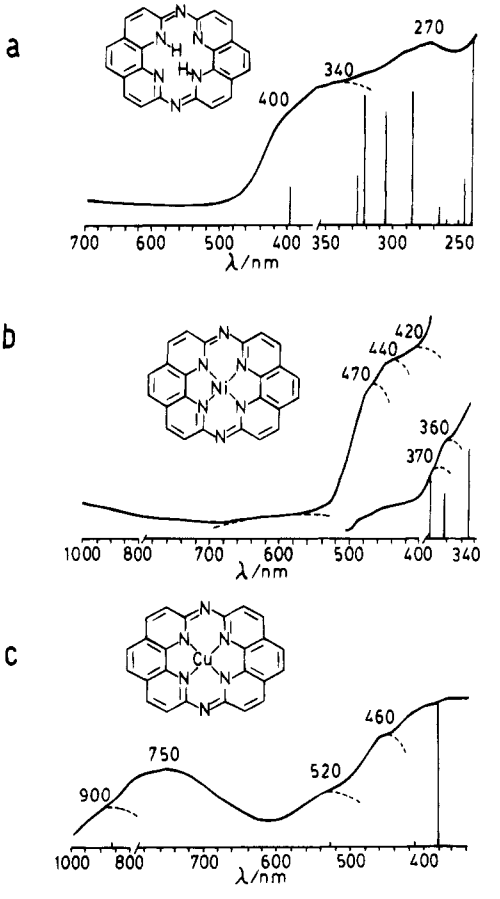


**Figure 2.** Electronic spectra: (a) Hexaazacyclophane base; (b) Ni complex; (c) Cu complex. The spectra were recorded on a Karl Seiss Model DMR22 and on a Perkin-Elmer Model Cary-17. Vertical lines correspond to allowed calculated transitions.

(49) Ogawa, S.; Yamaguchi, T.; Gotoh, N. *J. Chem. Soc., Perkin. Trans.* **1974,** 976, **1972,** 577.
(50) Ogawa, S. *J. Chem. Soc., Perkin. Trans.* **1977,** 214.
(51) Seno, M.; Tsuchiya, S.; Ogawa, S. *J. Am. Chem. Soc.* **1977,** *99,* 3014.
(52) Zickendrakt, C.; Koller, E. J. USA Pat. 2, 897, 207, July 28, 1959, 897, 207.
(53) Halcrow, B. E.; Kermack, W. O. *J. Chem. Soc.* ***1946,*** 155.
(54) Costamagna, J.; Vargas, J.; Latorre, R.; Alvarado, A.; Mena, G. *Coord. Chem. Rev.* **1992,** *119,* 67.
(55) Martin, L. Y.; Sperati, R.; Busch, D. H. *J. Am. Chem. Soc.* **1977,** *99,* 2968.
(56) Sadasivan, N.; Endicott, J. E. *J. Am. Chem. Soc.* **1966,** *88,* 5468.
(57) Zerner, M. C. ZINDO Package, Quantum Theory Project, University of Florida, Gainesville, FL.

The geometry of the structures has been optimized by gradient techniques[58-60] (INDO/1 parametrization), mainly searching for the planarity and multiplicity ($M$) of the metal complexes. Changes in the N−N bond lengths, which determine the size of the *central hole* in porphyrin-like systems and influence in this way the reactivity, have been carefuly considered.

The experimental information on the ground state symmetry[22] indicates low-spin structures (diamagnetic) for both the ligand and the Ni complex, while the magnetic moment of the Cu complex has been found to be 1.85 $\mu_B$. We have compared the energy of the ground state with those of intermediate spin (triplet and quartet, respectively). In the case of the ligand the geometry of the singlet was fully optimized. The geometry of the triplet was frozen to that of the singlet in order to evaluate its stability. Singlet Ni and doublet Cu complex geometries were also fully optimized. Geometry optimizations of the triplet Ni and quartet Cu complexes were performed under $C_{2v}$ constraints to analyze the possibility of the out of plane motion of the central atom. Although a full optimization would be possible for each of the M, it leads to distortions that obscure the analysis of the orbitals involved in the excitations. As it is traditional to keep the $D_{4h}$ symmetry in porphyrin chemistry, we have used $D_{2h}$ (or $C_{2v}$) symmetry for the hexaazacyclophane compounds. The orbitals have been labeled according to these symmetries.

The SCF calculations just described were followed by a CI using a Rumer diagram technique[61] within the INDO/S, parametrized for spectroscopy. According to the parametrization of the method, only single excitations were included in each of the CIs. The single excitations were generated using nearly all of the $\pi$ molecular orbitals and all the d orbitals for each of the structures analyzed. The resulting CI consist of more than 80 (100 for the Me complexes) configurations in each of the 8 irreducible representations of $D_{2h}$. The oscillator strengths were evaluated with the dipole length operator, including all one center terms.[13] Not only for the spectroscopic transitions but also for the calculations of the electronic properties has the electronic correlation been included.

The calculations have been extended to porphyrin and its Ni and Cu complexes in order to establish a comparison of the structural characteristics and electronic spectra. When we worked with open shell structures for the doublet copper complex, an average operator[62] defined by one valence electron distributed in four orbitals was required, in order to preserve the symmetry of the molecular orbitals (MO). The orbitals from the average operator form the reference for a subsequent projection over pure spin states by means of a Rumer CI.[61]

It has been reported that the INDO model reproduces excitation energies of transitions below 40 000 $cm^{-1}$ within 2000 $cm^{-1}$ at the CIS level, with some shift from the experimental values for the charge transfer and particularly good reproducibility of the d → d transitions. The present calculations become a new test of the INDO/S accuracy, as we are comparing the calculated data with the experimental spectra. Because of the level of theory employed, the transition moments may be rather large for strongly allowed bands, although reasonably accurate for weaker transitions.

## 3. Ground State Structures

**3.1. Hexaazacyclophane (Hp).** The geometry of the hexaazacyclophane has been fully optimized without imposing any symmetry. $D_{2h}$ symmetry results from the calculations, starting from a geometry constructed on the basis of X-ray experimental interatomic distances.[63] The relative stability of the tautomeric isomers, corresponding to the H atoms bonded to the phenanthrene nitrogens or the N atoms 7, 23 (Figure 1), favors by 0.686 eV the former. The $D_{2h}$ symmetry implies the same distance from each of the H atoms to the chelating nitrogens on one phenanthrene moiety and is compatible with the delocalized structure depicted in Figure 1. Although an ionic interaction has been postulated,[28] the separation of the charge (−0.276 on the N, +0.243 on the H) is only indicative of a polar bond. The local charge density is mainly concentrated on the N atoms 7, 23, due to the $sp^2$ character of the lone pair electron, which is resonant between p and $sp^2$ in the chelating Ns. Results are in agreement with XPS spectra, where two N1s peaks separated 1.50 eV, with relative intensities 1:2, are observed. This is also supported by IR and NMR determinations and defines a difference with the porphyrin base, where each of the H atoms are localized on one of the central nitrogens, with a reduction of the $D_{4h}$ symmetry of the porphyrinate ion to $D_{2h}$.

The tetradentate ligands defined by these macrocycles, as is the case of porphyrins, have the capability to coordinate with a central metal atom by means of a $\sigma$ coordination of the N lone pairs with the metal together with a $\pi$ interaction of metal p$\pi$ and d$\pi$ with N p$\pi$ orbitals. The strengths of these interactions determine the electronic density on the metal atom, influencing, thence, the photo and catalytic activity. The reactivity of the metal center will depend, on the other hand, on the Me−N bond length, which also defines the ligand field strength. *The size of the hole,* defined by the chelating N atoms, appears, thence, as a parameter related to reactivity. It has been determined that a stronger ligand field is generated by the phthallocyanine, with a smaller indole N−metal distance than its porphyrin homologue. Because it is mainly determined by the interatomic N−N distance in the phenanthrene structure, the *size of the hole* in these structures is considerably smaller than that in porphyrins. After a full optimization of the structure of the porphyrin base, in the same conditions used for the hexaazacyclophane, we have found a distance from the chelating N atom to the center of 2.041 Å, 0.213 A larger than that in the hexaaza base. This would be indicative of a higher ligand field strength in the latter, which cannot be associated with a different local charge density on the chelating N atoms (-0.337 in the hexaaza, −0.365 in the porphyne dianions). Although the local charge density in pyrrole is known to be larger than on pyridine,[64] delocalization of the N electron pairs plays a major role in these structures.

Magnetic susceptibility measurements are consistent with a closed shell structure for the hexaaza macrocycle. Our calculated SCF/CI energies indicate that the ground state (GS) is a singlet $^1A_g$ ($b_{2g}^2$ $b_{1u}^2$ in the outer electrons). Because the LUMO, LUMO + 1, and LUMO + 2 are very close in energy (0.02 and 0.15 eV, respectively), whereas the HOMO and HOMO − 1 are separated by 0.14 eV (Figure 3), several excited states almost degenerate result from the calculations. For the occupation of two orbitals with one electron each, the high-spin configurations are favored, and the first three excited states correspond to $^3B_{2u}$ ($b_{2g}^2$ $b_{1u}^1$ $b_{3g}^1$), $^3B_{3u}$ ($b_{3g}^2$ $b_{2g}^1$ $b_{1u}^2$ $b_{1u}^1$), and $^3B_{1g}$ ($b_{2g}^2$ $b_{1u}^1$ $a_u^1$), which lie 2.20, 2.22, and 2.25 eV above the ground state energy. The first excited singlet, $^1B_{1g}$ ($b_{2g}^2$ $b_{1u}^1$ $a_u^1$) lies 2.78 eV over the GS and above about 0.50 eV from the low-lying triplets.

**3.2. Nickel Complex (Ni−Hp).** As was done for the ligand, the structure of the Ni complex has been fully optimized without symmetry constraints. The $D_{2h}$ symmetry is maintained, without significant change in the geometry. The bond lengths remain the same within 0.005 Å, while the N−Ni distance is 1.839 Å,

(58) Szabo, A.; Ostlund, N. S. *Modern Quantum Chemistry. Introduction to Advanced Electronic Structure Theory*; McGraw Hill: New York, 1989.
(59) Head, J. D.; Zerner, M. C. *Chem. Phys. Lett.* **1985,** *122,* 264.
(60) Head, J. D.; Zerner, M. C. *Chem. Phys. Lett.* **1986,** *131,* 359.
(61) Pauncz, R. *Spin Eigenfunctions*; Plenum Press: New York, 1979.
(62) (a) Zerner, M. C. *Int. J. Quant. Chem.* **1989,** *35,* 567. (b) Edwards, W. D.; Zerner, M. C. *Theoret. Chim. Acta* **1987,** *72,* 347.
(63) *Tables of Interatomic distances and Configurations in Molecules and Ions;* Sutton, L. E., Scientific Ed.; Special Publication No. 11; The Chemical Society: Burlington House, W, London, 1958.
(64) Heterocyclic Compounds, *Comprehensive Organic Chemistry,* Vol. 4; Sammes, P. G., Ed.; Pergamon Press: New York, 1979.

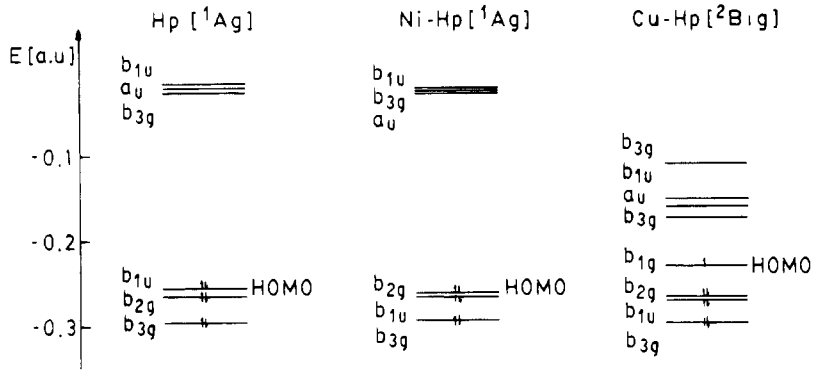


**Figure 3.** Molecular orbital distribution near the HOMO−LUMO gap for the hexaazacyclophane (Hp) and its Ni (Ni−Hp) and Cu (Cu−Hp) complexes. There are 16 extra unoccupied orbitals for the latter below 0.0 au.

**Table 1.** Mulliken Populations in the Chelating N Atoms (Columns 4, 6) and Metal Centers (Columns 3, 5) in the Ni and Cu Hexaazacyclophane (Ni−Hp, Cu−Hp) Complexes[a]

| A.O. | N($Hp^{-2}$) | Ni($^1$NiHp) | N($^1$NiHp) | Cu($^2$CuHp) | N($^2$CuHp) |
|---|---|---|---|---|---|
| s | 1.609 | 0.533 | 1.354 | 0.566 | 1.383 |
| $p_x$ | 1.123 | 0.409 | 1.103 | 0.422 | 1.101 |
| $p_y$ | 1.300 | 0.370 | 1.224 | 0.384 | 1.228 |
| $p_z$ | 1.305 | 0.121 | 1.490 | 0.131 | 1.493 |
| $d_{z^2}$ | | 1.903 | | 1.911 | |
| $d_{x^2-y^2}$ | | 1.983 | | 1.981 | |
| $d_{xy}$ | | 0.762 | | 1.488 | |
| $d_{xz}$ | | 1.986 | | 1.990 | |
| $d_{yz}$ | | 1.969 | | 1.982 | |

[a] The superindex gives the ground state M of each compound. The second column gives the populations on the N atom in the dianionic hexaazacyclophane ligand. The populations in the $Ni^{2+}$ ion are 1.0, 2.0, 1.0, 2.0, and 2.0 for the $d_{z^2}$, $d_{x^2-y^2}$, $d_{xy}$, $d_{xz}$, and $d_{yz}$ orbitals, respectively, while they are 2.0, 2.0, 1.0, 2.0, and 2.0 for the same orbitals of the $Cu^{2+}$ ion.

**Table 2.** Mulliken Populations in the Chelating Nitrogen Atoms (Columns 4, 6) and Metal Centers (Columns 3, 5) in the Ni and Cu Porphyrin Complexes (NiP, CuP)[a]

| A.O. | N($P^{2-}$) | Ni($^1$NiP) | N($^1$NiP) | Cu($^2$CuP) | N($^2$CuP) |
|---|---|---|---|---|---|
| s | 1.664 | 0.545 | 1.389 | 0.576 | 1.406 |
| $p_x$ | 1.186 | 0.416 | 1.143 | 0.438 | 1.148 |
| $p_y$ | 1.348 | 0.416 | 1.143 | 0.438 | 1.148 |
| $p_z$ | 1.305 | 0.116 | 1.529 | 0.111 | 1.515 |
| $d_{z^2}$ | | 1.935 | | 1.935 | |
| $d_{x^2-y^2}$ | | 1.995 | | 1.994 | |
| $d_{xy}$ | | 0.583 | | 1.405 | |
| $d_{xz}$ | | 1.981 | | 1.983 | |
| $d_{yz}$ | | 1.981 | | 1.983 | |

[a] The superindex gives the ground state *M* of each compound. The second column gives the populations on the N atom in the dianionic porphyrinate ligand. The populations in the $Ni^{2+}$ ion are 1.0, 2.0, 1.0, 2.0, and 2.0 for the $d_{z^2}$, $d_{x^2-y^2}$, $d_{xy}$, $d_{xz}$, and $d_{yz}$ orbitals, respectively, while they are 2.0, 2.0, 1.0, 2.0, and 2.0 for the same orbitals of the $Cu^{2+}$ ion.

only 0.010 Å larger than the N-center distance in the ligand. This optimized structure was used in further calculations.

The analysis of the frontier orbitals shows several molecular orbitals very close in energy at both sides of the HOMO−LUMO gap (Figure 3). The HOMO and HOMO − 1 are separated by only 0.07 eV, while the LUMO and LUMO + 1 and the LUMO + 1 and LUMO + 2 are separated by 0.08 and 0.07 eV, respectively. The small energy differences lead to several almost degenerate calculated states of different *M*.

In agreement with XPS and magnetic susceptibility data,[28] we found a $^1A_g$ ($b_{1u}^2\ b_{2g}^2$ in the outer electrons) ground state, which is 2.69 eV more stable than the next singlet $^1B_{1g}$ ($b_{1u}^2\ b_{2g}^1\ b_{3g}^1$). There are at least five low-lying triplet states among them: $^3B_{3u}$ ($b_{1u}^2\ b_{2g}^1\ b_{1u}^1$), $^3B_{1g}$ ($b_{1u}^2\ b_{2g}^1\ b_{3g}^1$), $^3B_{2u}$ ($b_{1u}^2\ b_{2g}^1\ a_u^1$), $^3B_{1g}$ ($b_{1u}^1\ b_{2g}^2\ a_u$), and $^3A_g$ ($b_{1u}^1\ b_{2g}^2\ b_{1u}$), which are 1.86, 1.90, 2.19, 2.26, and 2.33 eV higher in energy than the singlet GS.

The HOMO ($b_{2g}$), doubly occupied in the singlet, is mainly $\pi$ in character, involving in the delocalized structure the $d_{xz}$ orbitals in the Ni atom.

A Mulliken population analysis after CI calculations (Table 1) shows a decrease in the population of the s, $p_x$, and $p_y$ (in plane) orbitals on the chelating N atoms, consistent with a $\sigma$ bond with charge transfer to the metal, together with an increase of the N $p_z$ population which denotes back-donation from the metal. The balance of both effects results in an increase of the population on the Ni atom, relative to the free $Ni^{2+}$, showing the larger importance of the $\sigma$ effect. The decrease of the Mulliken population on the $d_{xy}$ orbital is associated with its destabilization under the influence of the ligand field but does not change the global effect on the Ni atom, due to the parallel increase of the electronic population on the $d_{z^2}$ orbital. The decrease in the local charge density on the chelating N atoms, as well as the negative charge density on the Ni, is consistent with this effect (Figure 1). A similar interaction is found in the porphyrin (Table 2), where the local charge density on the N decreases but on $p_z$, and the $d_{xy}$ orbital is destabilized by the ligand field. The splitting of the orbitals, measured from the $d_{x^2-y^2}$ to the $d_{xy}$ orbital, is similar (0.41 and 0.43 au, respectively) for the hexaaza and the porphyrin complexes. The smaller charge density on the Ni atom in the porphyrin compared to the hexaaza complex can be explained on the basis of the smaller $\sigma$ charge transfer, which is distance dependent.

The geometry of the triplet, optimized under $C_{2v}$ symmetry to allow the out of plane shift of the metal atom, also retains the $D_{2h}$ symmetry. The interatomic distances in the ligand remain the same within 0.005 Å, increasing the Ni−N distance in 0.048 Å. The singly occupied HOMO ($a_u$) and HOMO − 1 ($b_{2g}$) orbitals, are also $\pi$ in character, although the HOMO does not involve the central metal. The $s^{0.5}pd^{8.5}$ electronic configuration in the Ni atom is the same for the singlet and for the triplet.

**3.3. Copper Complex (Cu−Hp).** In spite on the higher multiplicity ($M = 2$), which is known to favor out of plane geometries, $D_{2h}$ symmetry also results for the Cu complex after a full optimization under $C_{2v}$ constraints. The geometry changes in the same magnitude, relative to the hexaaza base, as it did in the Ni complex (Me−N distance equal to 1.839 Å). As previously stated for the Ni complex, the optimized structure was used in further calculations.

Because of the open shell structure, excited states are easily achieved by means of the promotion of the unpaired electron in the HOMO orbital to high-energy levels (Figure 3) rendering exited doublets, a process that requires less energy than that

associated with quartet states. While in the Ni complex (closed shell) it is always neccessary to uncouple electrons to obtain either singlet or triplet excited states, in the Cu complex no uncoupling of electrons is required for the lower energy excitations. The HOMO and HOMO − 1 are separated, on the other hand, by 0.82 eV, making the promotion of an inner electron, to give quartet states, highly unfavored compared with the promotion of an electron in the HOMO to give excited doublet states. The LUMO and LUMO + 1 are separated by 0.38 eV (0.20 between the LUMO + 1 and LUMO + 2), so that the degeneracy pattern characteristic of the Ni complex does not hold for the Cu one. Finally, the HOMO − 1 and HOMO − 2 are separated by only 0.07 eV, so that the promotion of an inner electron to generate either doublets or quartets gives rise to several close lying states.

According to the previous scheme there are three excited doublets above the ground state and below the lowest energy quartet, which correspond to the promotion of the unpaired electron in the HOMO to the LUMO, LUMO + 1, and LUMO + 2, respectively.

The ground state, $^2B_{1g}$ ($b_{1u}^2\, b_{2g}^2\, b_{1g}^1$), is calculated to be 1.10 eV more stable than the first excited doublet $^2B_{3g}$ ($b_{1u}^2\, b_{2g}^2\, b_{3g}^1$). The next excited doublet states are 1.49 and 1.79 eV higher in energy and correspond to $^2A_u$ ($b_{1u}^2\, b_{2g}^2\, a_u^1$) and $^2B_{1u}$ ($b_{1u}^2\, b_{2g}^2\, b_{1u}^1$) states, respectively. Higher energy states belong to the promotion of inner electrons to low-lying empty levels. Calculated CI energies for a given set of singly occupied orbitals $^{2,4}B_{2u}$ ($b_{1u}^2\, b_{2g}^1\, b_{1g}^1\, b_{2u}^1$), $^{2,4}A_g$ ($b_{1u}^2\, b_{2g}^1\, b_{1g}^1\, b_{3g}^1$) and frozen geometry (to that of the doublet) always give the quartet just below (about 0.04 eV) the doublet. Far from this simple analysis, the quartet state of the Cu complex is structurally interesting by itself. The optimization of the geometry under $C_{2v}$ symmetry favors an out of plane movement of the Cu atom which defines, together with the chelating N atoms, a central square pyramid of 0.517 Å height. This geometry optimization splits the doublet and quartet states, leading to a most stable quartet, 3.81 eV above the doublet ground state.

A Mulliken population analysis shows a similar interaction pattern as was previously described for the Ni complex (Table 1), mainly associated with $\sigma$ N−Cu bonds with some donating character to the metal. The $d_{xy}$ orbital is not as strongly destabilized, as in the Ni complex, (0.16 au from the $d_{x^2-y^2}$), and defines a partially filled HOMO orbital. The unpaired electron is thence, localized on the metal atom. The same pattern is found in the Cu porphyrins, where the unpaired electron is localized in the HOMO $d_{xy}$ orbital, which is destabilized 0.23 au relative to the $d_{x^2-y^2}$.

For both the Ni and Cu porphyrin and hexaazacyclophane complexes, the splitting of the d orbitals under the $D_{2h}$ field, for the $d_{xy}$ orbital pointing toward the chelating N atoms, follows the pattern shown in Figure 4.

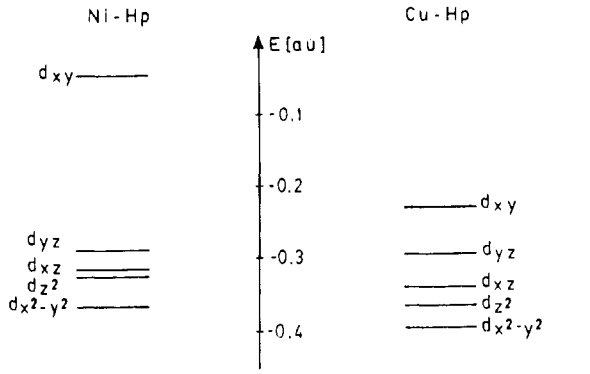


**Figure 4.** Splitting of the d orbitals of the $Ni^{2+}$ ($d^8$) and $Cu^{2+}$ ($d^9$) cations under the influence of the $D_{2h}$ field.

**Table 3.** Free Base Porphyrin Energies As Predicted by Gouterman[11] and Calculated in the Present Work (H's along *y* Axis)[a]

| | from ref 11 | | | this work | | | |
|---|---|---|---|---|---|---|---|
| | $E$ (cm$^{-1}$) | $\lambda$ (nm) | $f$ | $E$ (cm$^{-1}$) | $\lambda$ (nm) | $f$ | pol |
| Q | 13 743 | 728 | 0.031 | 13 588.0 | 735.9 | 0.021 | *y* |
| | 17 518 | 571 | 0.006 | 16 338.2 | 612.1 | 0.034 | *x* |
| B | 25 171 | 397 | 0.510 | 26 619.8 | 375.7 | 1.687 | *y* |
| | 28 603 | 349 | 2.830 | 27 689.6 | 361.1 | 2.338 | *x* |
| N | 30 820 | 324 | 3.010 | 32 465.0 | 308.0 | 1.272 | *y* |
| | 33 164 | 302 | 0.380 | 35 241.8 | 283.8 | 0.315 | *x* |
| | | | | 38 291.4 | 261.2 | 0.158 | *y* |
| | | | | 40 227.3 | 248.6 | 0.222 | *x* |
| L | 42 887 | 233 | 0.060 | 42 899.9 | 233.1 | 0.075 | *y* |
| | 42 412 | 236 | 0.065 | 40 921.3 | 244.4 | 0.009 | *x* |
| | 44 329 | 226 | 0.340 | 43 856.8 | 228.0 | 0.328 | *y* |
| | 47 625 | 210 | 0.007 | 44 014.9 | 227.2 | 0.017 | *x* |

[a] When a Ni atom is complexed, the Q band appears at 634 nm and the B band is hypsochromically shifted to 354.6 nm, whereas no significant change is associated with the N and L bands, which are fused to a single feature at 286.5 and 252 nm, respectively. Oscillator strengths ($f$) and polarization of the transitions (pol) are also included.

## 4. UV−Visible Spectroscopy

**4.1. Hexaaza Macrocycle (Ligand).** Many research articles deal with the spectra of porphyrin complexes, which are largely composed, in the high-energy region, of $\pi \rightarrow \pi^*$ transitions. The low-energy region of the spectra has been largely studied to analyze the origin of their photo and catalytic reactivity and is usually described in terms of a Q band in the visible, with a broad vibrational structure, and an intense B (Soret) band (~400 nm) in the near-UV.[1,8,10,11] Substitutions in the ligand shift the Q and B bands, whose position is also dependent on the metal tetracoordinated to the pyrrolic Ns. It is known that the Soret band shifts hypsochromically into the 330 nm region in the case of aza substitution,[3] while bands in the visible undergo a significant bathochromic shift. Significant shifts are also associated with benzo substitution.

In spite of the wealth of information related to the low-energy region of substitued porphyrins, not so much concern has been focused on the high-energy region, which is also of interest when a new ligand is analyzed. Gouterman[10,11] was the first to analyze the high-energy side of the spectra, naming two weakly allowed configurations close to the Soret band as N and L transitions.

In order to decide whether or not we can separate in Q, B, N, and L assignments the bands of the hexaazacyclophane (Hp), we have compared our calculated spectra with that of free base porphyrin, for which the previously mentioned bands have been defined.

As has been previously reported by Gouterman,[10,11] we have found, for the free base porphyrin, four sets of split bands corresponding to transitions from the HOMO (Q band), HOMO − 1 (B band), and inner orbitals to the $b_{3g}$ and $b_{2g}$ orbitals, almost degenerate, that belong to the splitting of the $e_g$ (LUMO) in the porphyrinate, when the symmetry is reduced to $D_{2h}$ in the free base (Table 3). The origin of the Q and B bands has been explained on the basis of the four orbital model,[1] which considers the transitions from the $a_{1u}$, $a_{2u}$ orbitals, in $D_{4h}$ symmetry ($b_{1u}$, $a_u$ in $D_{2h}$), to either the $e_g$ or the $b_{2g}$, $b_{3g}$ orbitals that result after reduction of the $D_{4h}$ symmetry. There is a clear separation in energy between the HOMO and HOMO − 1 in the free porphyrin base (of $D_{2h}$ symmetry) and the inner orbitals (1.88 eV) as well as between the LUMO + 1 and LUMO + 2

**Table 4.** INDO/S−CI−S Calculated Excited States of the Hexaazacyclophane Base[a]

| state | dominant conf and coeff sq | ΔE ($cm^{-1}$) | ΔE (nm) | *f* | pol | label | exp |
|---|---|---|---|---|---|---|---|
| $^1B_{2u}$ | $(b_{2g},a_u)$ 0.25, $(b_{1u}, b_{3g})$ 0.60 | 25 184 | 397.1 | 0.283 | *y* | Q ($\pi \rightarrow \pi$) | 400 |
| $^1B_{1u}$ | $(b_{1g},a_u)$ 0.46, $(b_{2u},b_{3g})$ 0.39 | 26 547 | 376.7 | 0.018 | z | $\pi \rightarrow \pi$ | |
| $^1B_{3u}$ | $(b_{2g},b_{1u})$ 0.73 | 30 434 | 328.6 | 0.355 | *x* | Q ($\pi \rightarrow \pi$) | |
| $^1B_{2u}$ | $(b_{2g},a_u)$ 0.59, $(b_{1u},b_{3g})$ 0.31 | 30 992 | 322.7 | 0.883 | *y* | B ($\pi \rightarrow \pi$) | 340 |
| $^1B_{2u}$ | $(b_{1u},b_{3g})$ 0.74 | 32 641 | 306.4 | 0.747 | *y* | $\pi \rightarrow \pi$ | |
| $^1B_{3u}$ | $(b_{3g},a_u)$ 0.38, $(b_{1u},b_{2g})$ 0.47 | 35 102 | 284.9 | 0.910 | *x* | B ($\pi \rightarrow \pi$) | 270 |
| $^1B_{1u}$ | $(b_{1g},a_u)$ 0.35, $(b_{2u},b_{3g})$ 0.46 | 35 826 | 279.1 | 0.003 | *z* | $\pi \rightarrow \pi$ | |
| $^1B_{2u}$ | $(b_{2g},a_u)$ 0.19, $(b_{1u},b_{3g})$ 0.56 | 37 623 | 265.8 | 0.137 | *y* | $\pi \rightarrow \pi$ | |
| $^1B_{3u}$ | $(b_{3g},a_u)$ 0.48, $(b_{1u},b_{2g})$ 0.29 | 38 551 | 259.4 | 0.002 | *x* | $\pi \rightarrow \pi$ | |
| $^1B_{3u}$ | $(b_{3g},a_u)$ 0.48, $(b_{1u},b_{2g})$ 0.37 | 39 604 | 252.5 | 0.030 | *x* | $\pi \rightarrow \pi$ | |
| $^1B_{2u}$ | $(b_{2g},a_u)$ 0.59, $(b_{1u},b_{3g})$ 0.23 | 40 459 | 247.2 | 0.281 | *y* | $\pi \rightarrow \pi$ | |
| $^1B_{3u}$ | $(b_{3g},a_u)$ 0.21, $(b_{1u},b_{2g})$ 0.62 | 41 151 | 243.0 | 1.223 | *x* | $\pi \rightarrow \pi$ | 240 |
| $^1B_{1u}$ | $(b_{1u},a_g)$ 0.49, $(b_{3u},b_{2g})$ 0.37 | 43 476 | 230.0 | 0.044 | *z* | $\pi \rightarrow \pi$ | |
| $^1B_{3u}$ | $(b_{2g},b_{1u})$0.42, $(b_{3g},a_u)$ 0.27 | 45 436 | 220.1 | 0.511 | *x* | $\pi \rightarrow \pi$ | |

[a] Ground state $^1A_g$. Only those transitions with nonzero oscillator strength (*f*) are given. Polarization of the transitions (pol) is also included. MO notation corresponds to $D_{2h}$ symmetry. Q and B assignments are discussed in the text.

(1.68 eV). The four orbital picture is, thence, particularly appropriate for the description of the transitions.

In the hexaazacyclophane, the $\pi$ electrons are more efficiently delocalized in the fused benzene rings. Being, at the same time, a larger system, there are several close-lying molecular orbitals near the HOMO−LUMO gap. The near degeneracy of the orbitals previously described (section 3) does not allow us to separate transitions to the LUMO and LUMO + 1 from those to LUMO + 2. On the other hand, on the basis of group theory, not the LUMO, $b_{3g}$, and LUMO + 1, $a_u$, but the LUMO and LUMO + 3 ($b_{3g}$ and $b_{2g}$, respectively) are related to a split $e_g$ in $D_{4h}$ symmetry. These considerations clearly demonstrate that the four orbital model cannot be applied. Besides, there is no band in the visible that can be labeled "Q".

The calculated transitions from the ground state $^1A_g$ are given in Table 4. Together with the excitation energies and oscillator strengths, the dominant configurations and corresponding excited states are shown to help analyze the major type of excitation involved in the observed transition. There are 14 bands in the energy range where the Q, B, N, and L bands appear for the free base porphyrin. Because of the symmetry of the orbitals, transitions to the LUMO−LUMO + 1 cannot be associated with transitions to a split $e_g$. However if, on the consideration of the MOs involved in the transitions, we label Q and B bands as indicate in Table 4, there is an hypsochromical shift of the B band, relative to the typical value, close to 400 nm, characteristic of aza substitution. The characteristic hypsochromic shift that accompanies the aza substitution is explained on the basis of the increase of the electronegativity when the carbon atoms are bonded to the more electronegative N in a link N−C−N−C−N. This effect counterbalances the larger extension of the resonant system.

To help understand the position of the bands, we have calculated the spectra of tetraazaphenanthrene, substituting the N atoms 7, 23 (Figure 1) by CH groups. The bands are bathochromically shifted in 40 nm, in agreement with the hypsochromical shift associated with the introduction of electronegative groups. We have compared, on the other hand, the spectra of 1,10-diazaphenanthrene, where the lowest energy band appears at 330 nm. The bathochromic effect in going from diaza to tetraazaphenanthrene can be understood on the basis of the increase of the delocalization of the $\pi$ electrons, as it is known that succesive annulations shift the $\pi \rightarrow \pi^*$ bands to lower frequencies.[64] To complete the scheme, the lower energy bands of quinoline (313 nm)[65] can be included in the comparison to exemplify the effect of annulation.

The spectrum of the hexaazacyclophane base is, on the whole, substantially different from that of porphyrin base, but it is of interest to analyze them comparatively in the effect produced by the introduction of a transition metal, chelated by the four N atoms, in the center of both structures.

In Table 4 the calculated spectrum is compared to the experimental one, where the bands at lower energy appear as shoulders of the high-energy intense peak at 270 nm, which is associated with the one calculated at 243 nm.

**4.2. Nickel Complex (Ni−Hp).** The earlier comparisons of the UV−visible spectra of different metalloporphyrins have lead to the conclusion that the wavelength of the transitions decrease as the electron acceptor properties of the cations, which limit the conjugation in porphyrin, become more pronounced.[66] The total shift of a band is generated by different effects: s, charge transfer, steric, and backward p effect. According to the discussion of the ground state properties of the Ni complex (section 3.2), s and charge transfer effects are relevant and should result in hypsochromic shifts when going from the ligand to the complex.

The charge transfer is larger in the hexaazacyclophane than in its porphyrin analog. However, because of the larger delocalization of the charge in the system, the effect is not so easily seen.

The hypsochromic shift in Ni−porphyrin relative to free base porphyrin is mainly evident in the B band, which, together with the Q band, involves excitations of the outer, less tightly bound electrons. The shifting effect on the Q band is, however, obscured because a single feature of intermediate energy results, in $D_{4h}$ symmetry, from the overlap of the two bands which were initially separated 124 nm in the free base of $D_{2h}$ symmetry.

The effect is even less clear in the Ni−hexaazacyclophane. The $D_{2h}$ symmetry of the complex remains after chelation, with no overlap of the Q bands. Orbitals around the HOMO−LUMO gap have a large contribution on the metal center (Table 1, Figure 1) and are considerably affected by the ligand.

The net result upon chelation is not reflected in an important shift of the bands relative to the ligand but in a decrease of their intensity. A clear hypsochromic shift of the first (lowest energy) band belongs to the contribution of the inner electrons (HOMO − 2), not involved in transitions in the ligand. There is a pattern of bathochromic shifting in the bands of higher energy (322.7 nm, Table 4, to 334.1 nm, Table 5; 243.0 nm, Table 4, to 252.1 nm, Table 5), which involve excitations from HOMO − 1 or HOMO − 2 orbitals, $\pi$ in character, but largely localized on the metal center. The negative charge density on

(65) Mason, S. F. In *Physical Methods in Heterocyclic Chemistry;* Katritzky, A. R., Ed.; Academic Press: New York, 1963; Vol II, Chapter 7.

(66) Williams, R. *Chem. Rev.* **1956,** *56,* 299.

**Table 5.** INDO/S–CI–S Calculated Excited States of the Ni–Hexaazacyclophane ($^1A_g$ Ground State) Complex[a]

| state | dominant conf and coeff sq | $\Delta E$ ($cm^{-1}$) | $\Delta E$ (nm) | $f$ | pol | label | exp |
|---|---|---|---|---|---|---|---|
| $^1B_{1g}$ | ($b_{1g}$,$a_g$) 0.66, ($b_{1u}$,$a_u$) 0.13, ($b_{2g}$,$b_{3g}$) 0.11 | 21 786 | 459.8 | | | $d_{z^2} \rightarrow d_{xy}$ | 470 |
| $^1B_{3g}$ | ($b_{2g}$,$b_{1g}$) 0.79 | 21 967 | 455.2 | | | $d_{z^2} \rightarrow d_{xy}$ | 470 |
| $^1B_{1g}$ | ($b_{1g}$,$a_g$) 0.26, ($b_{1u}$,$a_u$) 0.37, ($b_{2g}$,$b_{3g}$) 0.25 | 22 862 | 437.4 | | | $d_{z^2} \rightarrow d_{xy}$ | 440 |
| $^1B_{2g}$ | ($b_{1g}$,$b_{3g}$) 0.85 | 23 940 | 417.7 | | | $d_{yz} \rightarrow d_{xy}$ | 420 |
| $^1B_{1g}$ | ($b_{1g}$,$a_g$) 0.89 | 26 941 | 378.9 | | | $d_{x^2y^2} \rightarrow d_{xy}$ | 370 |
| $^1B_{2u}$ | ($b_{2g}$,$a_u$) 0.44, ($b_{1u}$,$b_{3g}$) 0.48 | 25 724 | 388.7 | 0.393 | $y$ | Q? ($\pi \rightarrow \pi$) | |
| $^1B_{3u}$ | ($b_{1u}$,$b_{2g}$) 0.78 | 29 349 | 340.7 | 0.280 | $x$ | $\pi \rightarrow \pi$ | |
| $^1B_{2u}$ | ($b_{2g}$,$a_u$) 0.39, ($b_{1u}$,$b_{3g}$) 0.37 | 29 928 | 334.1 | 0.582 | $y$ | $\pi \rightarrow \pi$ | 360 |
| $^1B_{2u}$ | ($b_{1u}$,$b_{3g}$) 0.69 | 33 276 | 300.5 | 0.354 | $y$ | $\pi \rightarrow \pi$ | |
| $^1B_{3g}$ | ($b_{3g}$,$a_g$) 0.95 | 33 838 | 295.5 | | | $d_{z^2} \rightarrow \pi$ | |
| $^1B_{3u}$ | ($b_{3g}$,$a_u$) 0.50, ($b_{1u}$,$b_{2g}$) 0.37 | 34 872 | 286.8 | 0.575 | $x$ | $\pi \rightarrow \pi$ | |
| $^1B_{3u}$ | ($b_{3g}$,$a_u$) 0.25, ($b_{1u}$,$b_{2g}$) 0.51 | 37 157 | 269.1 | 0.529 | $x$ | $\pi \rightarrow \pi$ | |
| $^1B_{2u}$ | ($b_{2g}$,$a_u$) 0.72 | 37 237 | 268.6 | 0.403 | $y$ | $\pi \rightarrow \pi$ | |
| $^1B_{1u}$ | ($b_{1u}$,$a_g$) 0.65, ($b_{2u}$,$b_{3g}$) 0.25 | 37 759 | 264.8 | 0.014 | $z$ | $d^{z^2} \rightarrow \pi$ | |
| $^1B_{3u}$ | ($b_{3g}$,$a_u$) 0.39, ($b_{1u}$,$b_{2g}$) 0.33 | 38 294 | 261.1 | 0.125 | $x$ | $\pi \rightarrow \pi$ | |
| $^1B_{2u}$ | ($b_{2g}$,$a_u$) 0.58, ($b_{1u}$,$b_{3g}$) 0.18 | 39 574 | 252.7 | 0.476 | $y$ | $\pi \rightarrow \pi$ | 270[b] |
| $^1B_{3u}$ | ($b_{3g}$,$a_u$) 0.13, ($b_{1u}$,$b_{2g}$) 0.59 | 39 660 | 252.1 | 1.159 | $x$ | $\pi \rightarrow \pi$ | |
| $^1B_{3u}$ | ($b_{3g}$,$a_u$) 0.30, ($b_{1u}$,$b_{2g}$) 0.46 | 41 322 | 242.0 | 0.057 | $x$ | $\pi \rightarrow \pi$ | |
| $^1B_{3u}$ | ($b_{3g}$,$a_u$) 0.67, ($b_{1u}$,$b_{2g}$) 0.10 | 42 901 | 233.1 | 0.082 | $x$ | $\pi \rightarrow \pi$ | |
| $^1B_{2u}$ | ($b_{1u}$,$b_{3g}$) 0.69 | 43 713 | 228.8 | 0.067 | $y$ | $\pi \rightarrow \pi$ | |
| $^1B_{2u}$ | ($b_{2g}$,$a_u$) 0.25, ($b_{1u}$,$b_{3g}$) 0.45 | 48 054 | 208.1 | 0.478 | $y$ | $\pi \rightarrow \pi$ | |
| $^1B_{3u}$ | ($b_{2g}$,$b_{1u}$) 0.37, ($b_{3g}$,$a_u$) 0.29 | 48 273 | 207.2 | 0.744 | $x$ | $\pi \rightarrow \pi$ | |

[a] Only those $\pi \rightarrow \pi$ transitions with nonzero oscillator strength ($f$) are given. Polarization of the transition (pol) is also included. [b] Figure 2a.

the Ni atom may help one to understand the decrease in the availabily of the electrons, explaining in this way the bathochromic shift.

The inclusion of the metal atom not only shifts the ligand → ligand transitions by inductive effect. Two other type of transitions, d → d* and charge transfer (either metal to ligand or ligand to metal) excitations, become possible, although a clear distinction into types is destroyed in the presence of strong covalent bonding. The first class (d → d*) of transitions is forbidden in the atom or ion but gain intensity through spin orbit coupling between states of different *M*.

In the Ni complex d → d* excitations appear in the 360–470 nm region (Table 5). Although the 370 nm may be overlapped by the $\pi \rightarrow \pi^*$ transitions, the others are clearly associated with the 470, 440, and 420 nm features in the experimental spectrum. All d → d* transitions are g → g Laporte forbidden but might borrow intensity from close-lying bands through vibronic coupling. This is the case of the Ni–Hp complex, where the charge transfer transitions, although calculated with zero oscillator strength, can be assigned to the absorption bands in the low-energy region.

The lowest energy charge transfer excitation (295.5 nm) also overlaps with $\pi \rightarrow \pi^*$ transitions. Only one allowed charge transfer excitation, from the electron rich metal to the easily reduced unsaturated ligand, appears at 264.8 nm.

The last experimental feature that needs an interpretation is the band at 600 nm. Either d → d* or charge transfer excitations are calculated too high in energy to explain this extra peak. Although spin forbidden, calculated transitions from the singlet ground state to the lower energy triplets give rise to spectroscopic features in the 560–660 nm range. We assume that bands in this region belong to this kind of transition, which, actually being double excitations, can gain intensity through the mixing of the ground state with excited configurations, appearing as a noticeable feature in the experimental spectrum.

**4.3. Copper Complex (Cu–Hp).** The open shell structure of the Copper complex gives a particular complicated structure to the low-energy region of the spectrum, where several bands in the visible precede the characteristic $\pi \rightarrow \pi^*$ transition bands.

The lowest energy $\pi \rightarrow \pi^*$ band at 381.9 nm is hypsochromically shifted relative to the ligand, in the same magnitude and because of the same reason, as for the Ni complex. No bathochromic shift appears in the intermediate region of the spectrum (330–300 nm). This fact can be easily explained on the consideration of the smaller strength of the N–Cu compared to the N–Ni interaction, which is reflected in a smaller charge density on the Cu atom (Table 1). Although the $\pi$ orbitals involved in the excitations have a large contribution of the metal p orbitals, there is no concentration of the charge on the metal center able to justify a bathochromic effect similar to that in the Ni complex.

There is a characteristic feature in the low-energy region of the spectra, which is a band in the visible, of low coefficient, calculated as a $\pi \rightarrow \pi^*$ at 527.0 nm (Table 6) and associated with the experimental peak around 520 nm (Figure 2). The band is originated in transitions from the high occupied levels to the LUMO, without contributions of transitions to higher energy orbitals. The low-energy position of the band is justified by the different molecular orbital distribution and smaller HOMO–LUMO gap than in the Ni complex. The position of the band reseambles, for the first time, the Q band in porphyrins.

If the porphyrin analogy is made again for comparison, a hypsochromic shift of the Q and B bands relative to the free base, to 507.2 and 320.1 nm, respectively, results from the calculations on the doublet, planar porphyrin–Cu molecule. The large shift compared to the porphyrin–Ni compound cannot be easily explained on the basis of a $\sigma$ effect, as the charge transfer N → metal is larger in Ni–porphyrin than in Cu–porphyrin. On the other hand, it is difficult to correlate the behavior of complexes of open and closed shell structures, where the molecular orbital distribution around the HOMO–LUMO gap is different and so are the orbitals involved in the excitations.

In spite of the similarities of the intraligand bands, the low-energy region is characteristic of each of the complexes. Bands in the visible, at even lower energy than those in the Ni–Hp, develop in the Cu–Hp. These bands involve charge transfer excitations from the $d_{xy}$ orbital of the Cu atom (HOMO) to the lowest lying $\pi$ orbital in the ligand (giving a $Cu(II)^+$–$Hp^-$ complex) and are associated with bands in the spectra around 900, 750, and 460 nm. The calculated bands are hypsochromically shifted by about 50 nm relative to the experimental ones. The low-energy associated with these transitions is due to the characteristics of the HOMO orbital, together with the decrease of the HOMO–LUMO gap relative to the ligand. Charge

**Table 6.** INDO/S–CI–S Calculated Excited States of the Cu–Hexaazacyclophane ($^2B_{1g}$) Complex[a]

| state | dominant conf and coeff sq | $\Delta E$ ($cm^{-1}$) | $\Delta E$ (nm) | $f$ | pol | label | exp |
|---|---|---|---|---|---|---|---|
| $^2B_{3g}$ | $(b_{1g},b_{3g})$ 0.92 | 9 279 | 1077 | | | $d_{xy} \rightarrow \pi$ | |
| $^2A_u$ | $(a_u,b_{1g})$ 0.92 | 12 073 | 823.3 | 0.002 | | $d_{xy} \rightarrow \pi$ | 900 |
| $^2B_{1u}$ | $(b_{1g},b_{2u})$ 0.92 | 14 496 | 689.8 | 0.001 | $x$ | $d_{xy} \rightarrow \pi$ | 750 |
| $^2B_{3u}$ | $(b_{1u},b_{3g})$ 0.35 | 18 977 | 527.0 | 0.001 | $x$ | $\pi \rightarrow \pi$ | 520 |
| $^2A_u$ | $(b_{1g},a_u)$ 0.91 | 24 047 | 415.9 | 0.001 | | $d_{xy} \rightarrow \pi$ | 460 |
| $^2B_{3u}$ | $(b_{2g},a_u)$ 0.46, $(b_{1u},b_{3g})$ 0.52 | 26 182 | 381.9 | 0.370 | $x$ | $\pi \rightarrow \pi$ | |
| $^2B_{1u}$ | $(b_{1u},b_{1g})$ 0.91 | 26 441 | 378.2 | | | $d_{xy} \rightarrow p_z$ | |
| $^2A_g$ | $(b_{1g},a_g)$ 0.82 | 29 382 | 340.3 | | | $d_{xy} \rightarrow d_{z^2}$ | |
| $^2B_{2u}$ | $(b_{1u},b_{2g})$ 0.90 | 30 313 | 329.9 | 0.343 | $y$ | $\pi \rightarrow \pi$ | |
| $^2B_{3u}$ | $(b_{2g},a_u)$ 0.49, $(b_{1u},b_{3g})$ 0.45 | 31 201 | 320.5 | 0.737 | $x$ | $\pi \rightarrow \pi$ | |
| $^2B_{3u}$ | $(b_{1u},b_{3g})$ 0.78 | 33 859 | 295.3 | 0.483 | $x$ | $\pi \rightarrow \pi$ | |
| $^2B_{2u}$ | $(b_{3g},a_u)$ 0.55, $(b_{1u},b_{2g})$ 0.34 | 35 902 | 278.5 | 0.824 | $y$ | $\pi \rightarrow \pi$ | 270 |
| $^2B_{3u}$ | $(b_{1g},b_{3u})$ 0.91 | 37 391 | 267.4 | 0.100 | $x$ | $d_{xy} \rightarrow \pi$ | |
| $^2B_{3u}$ | $(b_{1u},b_{3g})$ 0.65, $(a_u,b_{2g})$ 0.20 | 38 104 | 262.4 | 0.114 | $x$ | $\pi \rightarrow \pi$ | |
| $^2B_{2u}$ | $(b_{3g},a_u)$ 0.77, $(b_{1u},b_{2g})$ 0.13 | 38 823 | 257.6 | 0.200 | $y$ | $\pi \rightarrow \pi$ | |
| $^2B_{2u}$ | $(b_{3g},a_u)$ 0.16, $(b_{1u},b_{2g})$ 0.10 | 39 078 | 255.9 | 0.034 | $y$ | $\pi \rightarrow \pi$ | |
| $^2B_{3u}$ | $(b_{2g},a_u)$ 0.57, $(b_{1u},b_{3g})$ 0.16 | 39 684 | 252.0 | 1.115 | $x$ | $\pi \rightarrow \pi$ | |
| $^2B_{3u}$ | $(b_{2g},a_u)$ 0.31, $(b_{1u},b_{3g})$ 0.11 | 40 160 | 249.0 | 0.114 | $x$ | $\pi \rightarrow \pi$ | |
| $^2B_{2u}$ | $(b_{3g},a_u)$ 0.26, $(b_{1u},b_{2g})$ 0.36 | 40 430 | 247.3 | 0.893 | $y$ | $\pi \rightarrow \pi$ | 240[b] |
| $^2B_{3u}$ | $(b_{1u},b_{3g})$ 0.14, $(b_{2g},a_u)$ 0.64 | 43 625 | 229.2 | 0.203 | $x$ | $\pi \rightarrow \pi$ | |

[a] For the $\pi$–$\pi^*$ transitions, only those with nonzero oscillator strength ($f$) are given. Polarization of the transitions (pol) is included. [b] Figure 2a.

transfer excitations of higher energy, as well as d → d* transitions, are hidden under the $\pi \rightarrow \pi^*$ bands.

## 5. Conclusions

The hexaazacyclophane ligand and its Ni and Cu complexes have been experimentally studied as porphyrin models, mainly in relation to the electrochemical reduction of $CO_2$. Because charge transfer is of major importance in these reactions, the origin of the electronic excitations of lower energy may help in understanding the nature of the redox processes, as well as whether it involves the ligand, the metal center, or both.

Using the INDO/S–CI method, we have accurately reproduced the transitions shown in the experimental UV–visible spectra. On the basis of the calculated transitions, we have associated the low-energy region of the spectra to d → d* transitions, in the case of the Ni complex, and to charge transfer (CT) ($d_{xy} \rightarrow$ L) excitations, in the case of the copper one. The existence of these CT and d → d* transition states at relatively low excitation energies indicates a possible participation of these transitions in the reduction mechanisms. From the increase of the electron density on the metal center, chelated by the Hp ligand (Table 1), which is larger than that associated with the porphyrin homolog (Table 2), we can infer a promising activity of the structures analyzed in this paper toward electrochemical reduction processes, which most likely would involve the metal center in the interaction. Present studies are focusing directly in the interaction of $CO_2$ with these complexes.

The analysis of the molecular orbital distribution, together with the comparison with that calculated for the porphyrin base, shows that a four orbital picture cannot be applied, and the intraligand bands cannot be labeled Q, B, N, and L, as they are for porphyrin.

The comparison of the shift in the $\pi \rightarrow \pi^*$ bands after metal complexing shows that no paralellism between these macrocycles and porphyrins can be established. The correlation between hypsochromical shifts and the strength of the $\sigma$(metal–N) bond cannot be held, on a molecular orbital basis, when open and closed shell structures, with a particular different molecular orbital distribution around the HOMO–LUMO gap, are considered.

**Acknowledgment.** A.H.J. is a member of the Research Career of CIC, and G.L.E. is a member of the Research Career of CONICET. The financial assistance of the Consejo Nacional de Investigaciones Científicas y Técnicas (CONICET), the Comisión de Investigaciones Científicas, CIC, Provincia de Buenos Aires, the Fundación Antorchas (Argentina), Fondo Nacional de Ciencias y Tecnología, FONDECYT, Project Pt0113/92, and the Dirección de Investigaciones Científicas y Tecnológicas, Universidad de Santiago de Chile y Dirección de Investigaciones, Universidad Metropolitana de Ciencias de la Educación (Chile) is gratefully acknowledged. This paper is dedicated to the celebration of the 65th birthday of Prof. Pedro J. Aymonino, Universidad de La Plata, La Plata, Argentina.

IC940440P